A COMPREHENSIVE ANALYSIS ON SIZING OF SOLAR ENERGY HARVESTER ELEMENTS FOR WIRELESS SENSOR MOTES

R.Hemalatha, R.Ramaprabha and S.Radha

SSN College of Engineering,

Chennai, 600117 - India

Emails: hemalathar@ssn.edu.in, ramaprabhar@ssn.edu.in, radhas@ssn.edu.in

Submitted: Nov. 1, 2014 ***Accepted: Jan. 14, 2015*** ***Published: Mar. 1, 2015***

Abstract- Wireless sensor networks (WSN) have limited lifetime due to on board battery. The lifetime can be improved by energy harvesting solutions. In this paper the solar energy harvester requirements for TelosB mote has been analyzed and calculated. Photovoltaic (PV) panel and battery sizing requirements are calculated by assuming that the mote follows SMAC and TDMA-MAC schedule for image communication. The calculations are validated by comparing it with the parameters calculated from the real time current consumption measurement of the mote. Lifetime has been predicted with the physical design of energy harvester. The analysis confirms that the lifetime of the network can be increased to a greater extent, by proper sizing of the harvester and efficient utilization of the available energy.

Index terms*:* WSN, energy harvester, lifetime prediction, battery, PV source

I. INTRODUCTION

In recent years WSN has gained importance and is used in a wide variety of applications such as military, environmental science, medical, space exploration, commercial applications etc. This improvement is mainly due to the drastic development in micro-sensor, microelectronics and wireless communication. They are capable of sensing, processing and communicating data to other devices [1]. As they are energized by battery, the lifetime of the motes are limited and is mainly dependent on the choice of application. It is also hard to locate the mote and replace it once it is dead. WSN is used for multimedia applications also [2], where the data rate for transmission is very high, so the life of the mote will extend only for a few days. Hence it is essential to use energy harvesting applications to power the mote.

The lifetime of the mote can be increased efficiently by using solar energy harvesting techniques than several other sources available in the outdoor environment, as solar cells have high power density [3]. The mote supplied by the harvester will use solar energy for processing, charging the battery when it is available and uses the battery power during its absence. The lifetime of the mote is based on current consumption of the mote at various states of operation and the duty cycle at which it is operated. The solar harvester has to be designed based on the need of applications. The PV panel and the battery size required will also change with the varying requirements. Hence it is essential to have an in-depth analysis on the sizing requirements of the elements of solar harvester. The performance monitoring of the distributed solar panels [27-29] can also be initiated to have a proper evaluation. There are a large number of PV harvesting circuits [3]-[5] and [10]-[12] proposed recently. Wide variety of MPPT algorithms [6], [8], [18], [23], [24] & [32] are used to gain better tracking accuracy. A low power maximum power point tracker using the adaptive maximum power point tracking (MPPT) algorithm suitable for WSN node is developed by Cesare Alippi [10]. They used current mode control and achieved power conversion efficiency in the range of 50 % - 60 %. DuraCap, a solar-powered energy harvesting system [11] used supercapacitor and lithium-ion batteries for energy storage. It also uses pulse frequency modulation (PFM) based regulator switching for multiple MPPT operation. Batteryless solar-harvesting circuit [14] is also proposed for low power applications but it is difficult to power the mote in cloudy and bad weather conditions. Ambimax system [12] tracked maximum power point (MPP) autonomously and used supercapacitors as backup at maximum efficiency. It

uses 70 mAh Li-polymer battery and two 10 F super capacitors as energy storage elements. It also utilizes multiple energy harvesting sources such as solar, wind, thermal, and vibration. Prometheus [38] used a MOS switch with simple dc-dc converter for power conversion. Harvested energy is stored in two stage energy storage consisting of two super capacitors in series and rechargeable lithium battery (200 mAh**).** In PV charger system [13] with SEPIC converter, peak current mode control is used with batteries as the storage element. The elements of the harvesting circuit are decided based on the solar panel and the battery used. Hoonki Kim et.al [19] proposed an energy harvesting circuit fabricated using a 0.35 μm CMOS process where MPPT circuit exploited a successive approximation register and a counter to solve the tradeoff problem between a fast transient response and a small steady-state oscillation with low-power consumption.

Based on the literature survey, all the harvesters have been designed by taking into account the general power consumption of WSN mote. The lifetime analysis of WSN with basic working principles has been discussed and they does not emphasize on the harvester sizing requirements. Alternatively, this paper aims at analyzing the energy consumption of the mote at different scenarios and to provide a methodology to device the range of the harvester elements to be used.

In this paper, TelosB mote has been considered for analysis, the duty cycle of the individual motes is determined by using SMAC (sensor-Medium Access Control) and TDMA (time division multiple access)-based MAC protocol [36]. Though there are efficient protocols available in literature [7], [31], [34], [37] & [39] the above mentioned protocols are used to determine the duty cycle, because PV panel and battery storage requirements can be estimated with worst case scenario. The choices made in this scenario will also be applicable for less energy consumption scenarios. Motes are assumed to follow the prescribed duty cycle. The lifetime of the battery operated mote is simulated and is compared with the lifetime of the energy harvester mote. In this paper, harvester energy requirement is obtained for different duty cycles and correspondingly the required panel ratings are calculated. The technical requirements of a solar energy harvester have been analyzed, which includes the efficiency calculation of the MPPT converter. The experimental verification of power consumption of the mote and the efficiency of the MPP tracker used in the energy harvester is evaluated. This enables the validation of the proposed analysis in real time.

This article is organized as follows; the mote taken for consideration and its power requirement in the different states of operation, energy consumption analyses of the mote while using different protocols are presented in Section II. The lifetime of the mote is estimated for varying duty cycles, without using harvester and is presented in Section III. Section IV describes the energy harvester designed and MPPT physical verification. It also gives the power losses associated with the converter and the efficiencies of individual blocks. In Section V, design requirements for the energy harvester are analyzed. The analysis is mote-specific. Panel sizing and the battery requirement are also presented. It also provides the experimental validation of the energy consumption analysis and compares the real time element requirements, from the theoretically derived data. Section VI discusses the lifetime analysis of the mote with energy harvester and Section VII provides the conclusion.

II. DETAILED ANALYSIS OF LOAD CHARACTERIZATION AND ENERGY CONSUMPTION

The typical WSN motes are battery operated and the processor in the mote consumes energy for computational tasks, the radio transceiver consumes more energy for transmitting the data towards the sink. The power consumption by the processor and the radio is dependent on the motes used. The mote used for lifetime analysis is TelosB [22] with TI MSP430 processor and CC2420 radio module. It has a data rate of 250 kbps.

The possible operational states of WSN mote are sleep, idle, transmit, receive and wakeup. As there is less power consumption during wakeup (as wakeup time is very less), it is assumed to be negligible for further calculations. The component status and current consumed by the TelosB mote [22] for different operational states are listed in the Table 1.The energy calculations can be further derived based on the time duration spent by the mote in the individual states.

Table 1: Mote Power Consumption

Mote State	**Component Status**		**Current Consumption**	
	Processor	**Radio module**	**Data sheet**	**Measured**
Sleep	Sleep	Sleep	5.1 μA	6.4 μA
Idle	Idle	Idle	18.8 mA	18 mA
Transmit (Tx)	On	Tx	19.5 mA	20 mA
Receive (Rx)	On	Rx	21.8 mA	23 mA

To enable real time analysis the mote is programmed to transmit 64 bytes of data. Programming is done in contiki with COOJA simulator. The real time current consumption of the mote in different operational states is measured as depicted in figure 1 and are listed in Table 1.

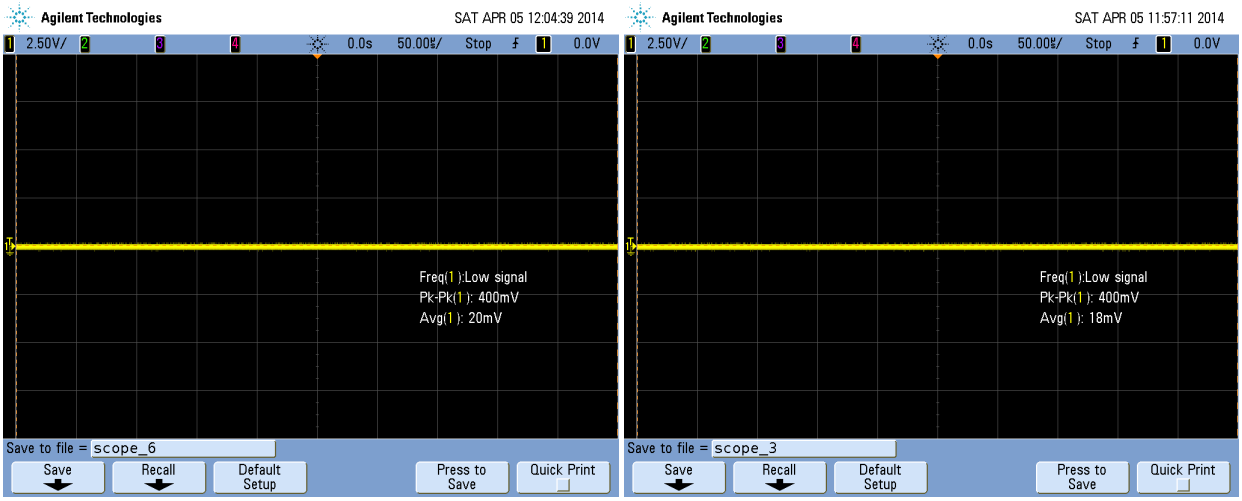

a) Transmit state b) Idle state

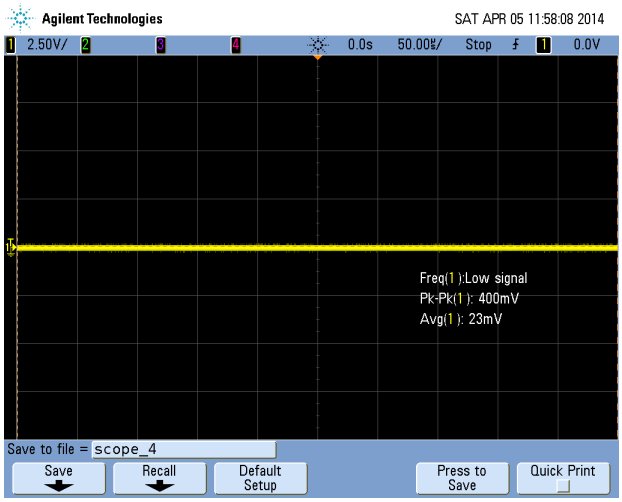

b) Receive state

Figure 1. Current measurement in different operation states

a. Case I: SMAC

SMAC protocol has a periodic wakeup-sleep pattern and adaptive listening. The major advantage of this protocol is less energy consumption and reduced synchronization overhead. It also avoids collision so that two interfering nodes will not transmit at the same time [36]. Based on the protocol the operational states of the mote have been considered. Many sensor network

applications assume that the nodes are in idle state for a long time, if no sensing of an event happens. This will increase the energy consumption considerably. Here, the listen time is reduced by allowing the mote to be in periodic sleep state, which introduces latency in the network. The energy consumption can be considerably reduced with the variation in the duty cycle. The states of operation of the mote using SMAC is shown in figure 2. Each node goes to sleep for some time, and then wakes up and listens to see if any other node wants to talk to it. During sleep, the node turns off its radio and sets a timer to awake itself later.

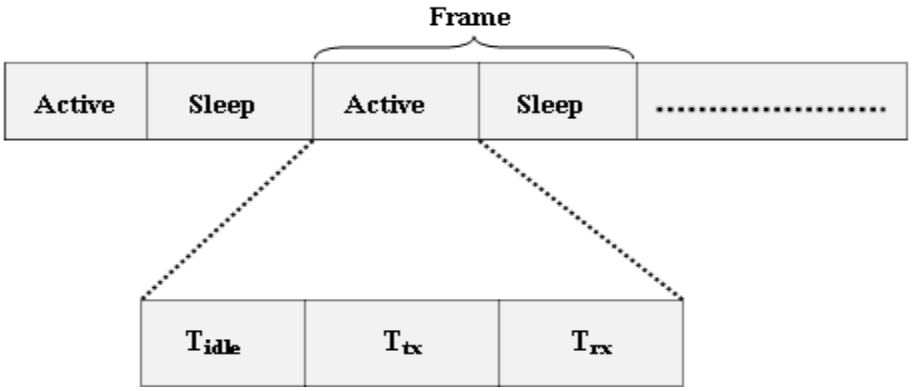

Figure 2. Time frame of Mote using SMAC protocol

The duration of time for active and sleep state can be selected according to different application scenarios. For simplicity these values are assumed to be same for all the nodes. The complete cycle of the active and sleep state is called a frame and the time period is given as,

$$T_{frame} = T_{active} + T_{sleep} \quad (1)$$

Duty cycle (D) in this case is given by

$$D = \frac{T_{active}}{T_{frame}} \quad (2)$$

where, $$T_{active} = T_{tx} + T_{rx} + T_{idle} \quad (3)$$

The mote is assumed to be idle, transmit and receive consecutively in active state. In reality the active state slot will not have fixed states of operation, as transmission and reception is dependent on the availability of the data in and towards the mote. The active slot usage has been formalized using Eqs. (1) to (3) to have a better energy analysis. The total energy consumed by the mote is calculated by Eq. (4). The sleep and active state energy is calculated using Eqs. (5) and (6).

$$E_{tot} = E_{sleep} + E_{active} \quad (4)$$

$$E_{sleep} = P_{sleep} \times T_{sleep} \quad (5)$$

$$E_{active} = \left(P_{tx} \times T_{tx}\right) + \left(P_{rx} \times T_{rx}\right) + \left(P_{idle} \times T_{idle}\right) \quad (6)$$

With the time frame adopted for duty cycle operation, the lifetime of the mote is calculated using Eq. (7).

$$Lifetime = \frac{Batterycapacity(mAhr)}{Currentconsumption\ of\ load(mA)} \quad (7)$$

The time to transmit is calculated by considering the packet structure used for transmission in the concerned platform as in Eq. (8).

$$T_{tx\_telosb} = \frac{\left(31 + P\right) \times 8}{datarate} \quad (8)$$

The MAC layer overhead for the packet transmission is considered as '31' for TelosB mote. P denotes the payload size. A default payload of 28 bytes [30], [17] is used in this paper. The number of packets transmitted is calculated based on the default payload size.

b. Case II: TDMA

This scenario utilizes TDMA schedule for energy and lifetime analysis. The time slot arrangement used in this study is shown in figure 3. Each user has an allotted specific slot within which they can transmit or receive, for the remaining time the user will be in sleep mode [36]. Assume there is 'n' number of nodes. All users will be in active state for the initial timeslot duration T_s which is called as the setup phase. In the setup phase the time slot assignment for the individual users will be finalized and it is fixed to avoid collisions to a greater extent. It also reduces the energy consumption as the user will be active during his allotted slot, the set up phase slot and remains in sleep state for the remaining duration. The slot allotted to the user will be wasted if it not has any data to be transmitted. Here the active state slot time allotted for i^{th} user is denoted by T_c and the slot allotted for the set up phase is denoted by T_s and is equal to one slot duration allotted for the individual user. In the active slot time the mote will be in transmit, receive or idle state and the setup phase is allotted for synchronization among all users.

The setup and steady state phases together are considered as a round. Single round length $\left(T_r\right)$ and the number of rounds $\left(N_r\right)$ in one day are calculated using Eq. (9) and (10)

$$T_r = \left(n \times T_c\right) + T_s \quad (9)$$

$$N_r = \frac{86400}{T_r} \tag{10}$$

Time duration that a single node will be in on, T_{on_r} and off, T_{off_r} state during one round is given by Eqs. (11), (13). Single round on time is the sum of the time duration allotted for an individual user and the set up phase. Usually the time allotted for the setup phase will be equal to the individual user slot duration.

$$T_{on\_r} = T_s + T_c \tag{11}$$

$$T_s = T_c = T_{tx} + T_{rx} + T_{idle} \tag{12}$$

$$T_{off\_r} = T_r - T_{on\_r} \tag{13}$$

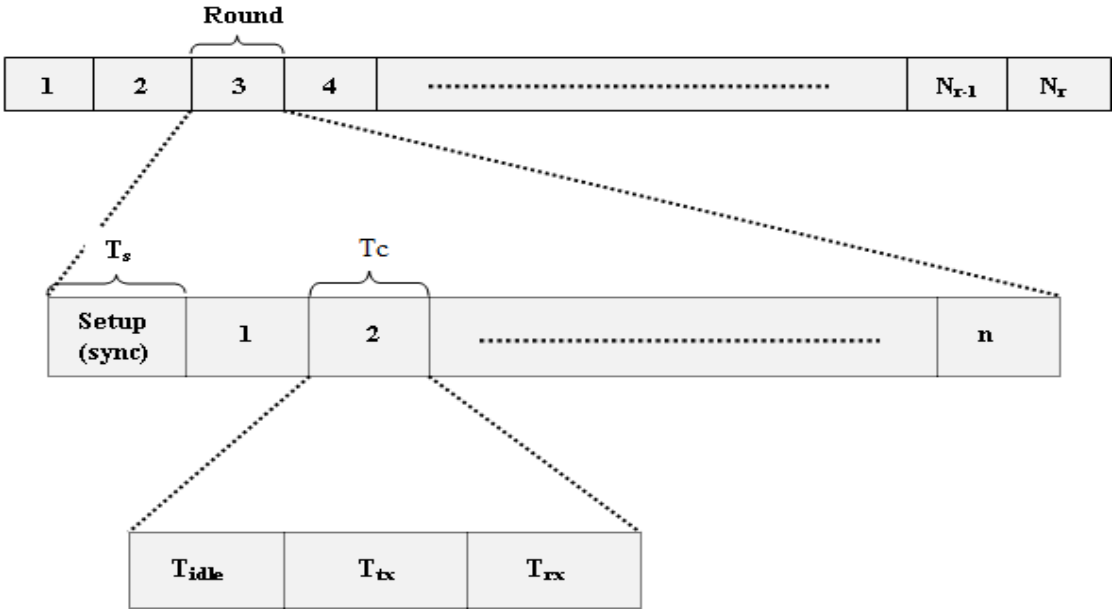

Figure 3. Time frame of Mote using TDMA protocol

Time duration that a single node will be on, T_{on_day} and off, T_{off_day} in a day is given as below in Eqs. (14) and (15). The energy consumed in the set up phase, in the individual slot duration and the energy consumed by the mote in one round and a day is calculated using Eqs. (16) to (18).

$$T_{on\_day} = T_{on\_r} \times N_r \tag{14}$$

$$T_{off\_day} = T_{off\_r} \times N_r \tag{15}$$

$$E_s = E_c = \left(P_{tx} \times T_{tx}\right) + \left(P_{rx} \times T_{rx}\right) + \left(P_{idle} \times T_{idle}\right) \quad (16)$$

$$E_{rd} = E_s + E_c + \left(P_{sleep} \times T_{off\_r}\right) \quad (17)$$

$$E_{day} = \left(E_s \times N_r\right) + \left(E_c \times N_r\right) + \left(P_{sleep} \times T_{off\_day}\right) \quad (18)$$

III. LIFETIME ANALYSIS WITHOUT ENERGY HARVESTER

Lifetime analysis is done using the parameters in the Table 1. and with the equations for each case as presented in the Section 2.

a. Case I: SMAC

Lifetime of the mote has been calculated for varying sleep duration using Eqs. (4) to (7). For the entire simulation the channel is assumed to be contention free. The parameters from Table 1 are used for the simulation. Sleep time is varied from 1s to 30 s, receive and idle time are considered as 5 ms and 3 ms respectively. The transmit time is dependent on the data length. The battery capacity considered for simulation is 300 mAhr. The life time calculations are done using MATLAB (R2011a) [25] and the results are shown in figure 4.

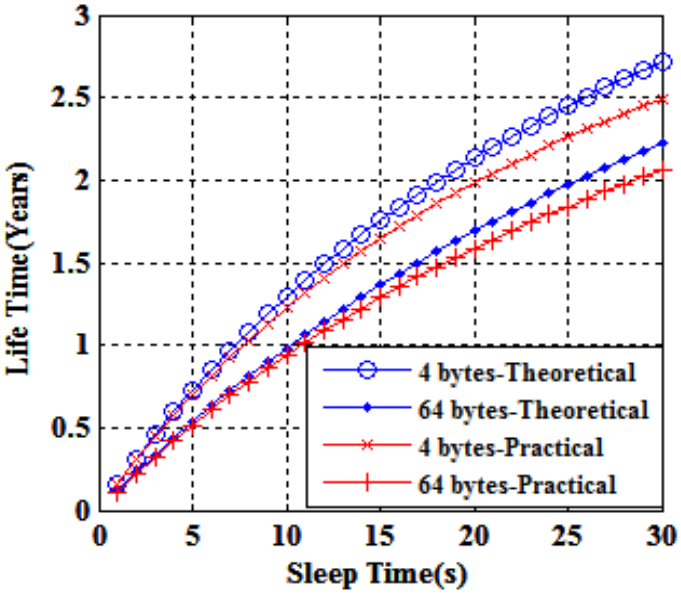

Figure 4. TelosB mote life time under varying Payload with SMAC schedule

With the increase in the sleep time the duty cycle decreases and the lifetime of the mote increases. The payload is considered as 4 and 64 bytes. It is chosen based on the assumption of an image application, transmitting a 2×2 and 8×8 raw image data. The lifetime of the TelosB mote decreases with the increase in payload that is to be transmitted. TelosB has reduced lifetime characteristics in the practical case as the current consumption is slightly greater than the data provided in the datasheet. The lifetime can further be increased by increasing the sleep time of the mote. But in real time deployment, the multimedia sensor networks have large amount of data to be transmitted in stipulated time, this will reduce the lifetime of the mote considerably if battery alone is used as the energy resource.

b. Case II: TDMA

The number of nodes (n) in the scenario is varied from 5 to 30. The simulation is performed with the parameters used in Case I except the sleep time which is varied based on the number of users. Lifetime estimation is done using Eqs. (9) to (18). The results are obtained for different duty cycles, the lifetime of the mote is plotted as shown in figure 5. When there is no activity to perform, the user is assumed to be in sleep mode in the setup phase and in his individual slot duration.

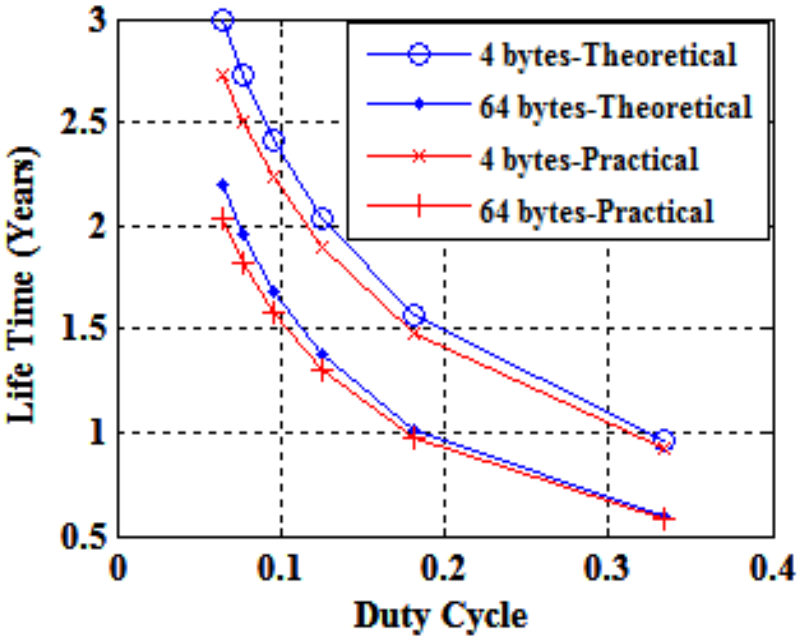

Figure 5. TelosB mote lifetime under varying Payload with TDMA-Mac schedule

With the Case II scenario, TelosB has reduced lifetime characteristics in real time case due to the increase in the measured current consumption.

IV. SYSTEM DESCRIPTION: SOLAR ENERGY HARVESTER

The solar energy harvester system used for the analysis is shown in figure 6. It consists of solar module, boost converter, battery, charge controller, buck converter to reduce the voltage down to the mote operating voltage and the WSN mote as the load [20].

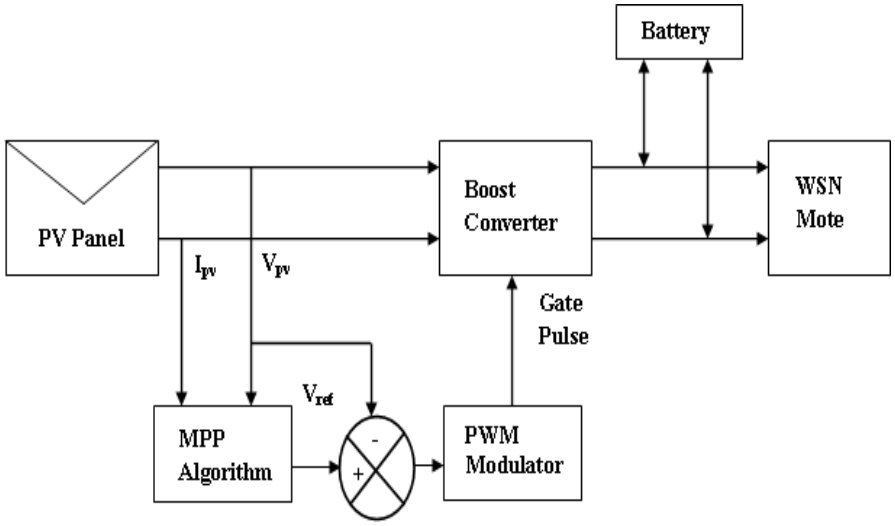

Figure 6. Solar Energy Harvester

The MPPT controller provides the peak operating point of the solar module whereas the boost converter provides the impedance matching with the battery and the solar module. The Blue Solar SL8585mm [9] PV panel is used. It provides a maximum power of 950 mW at standard test conditions. The boost converter [15] is designed with critical L = 107 mH and C = 123.29 μF, f_s = 5 kHz as the operating frequency of the converter and a voltage ripple of 5 %. Incremental conductance MPPT [35] algorithm is used. 4.8 V, 300 mAh Nickel metal hydride (NiMH) rechargeable battery is used as the storage element [26]. Battery charge control algorithm is used to prevent the battery from overcharging and extreme draining conditions. Buck regulator is used to provide the constant mote working voltage from the rechargeable battery. The detailed design and analysis of the harvester working is explained in [20] and is avoided here as the paper is

focused on the lifetime calculation. The experimental setup for verifying the MPPT and the results are presented in Fig. 7.

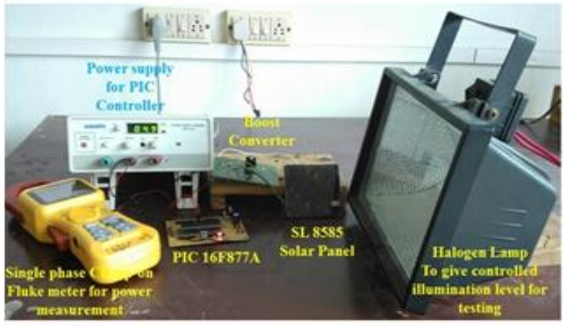

a)

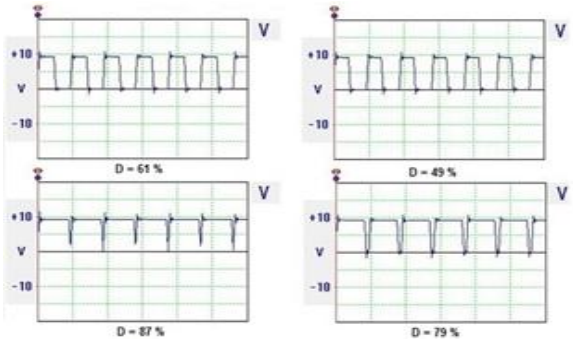

b)

Figure 7. (a) Experimental setup for MPPT circuit, (b) Gate pulse waveforms for different irradiance levels

The capability and working of the MPPT algorithm have been experimentally verified by varying insolation on the panel using halogen lamp. It is observed that the algorithm varies the pulse width to track the maximum power. These variations are shown in Fig. 7 (b).

The panel requirement for varying duty cycle is formulated with the inclusion of loss calculation associated with the boost converter. The power conversion efficiency can be increased by including this loss, while calculating the power budget for the requirement. The MPPT efficiency is calculated both in theoretical and experimental methods. The main losses in the converter are switching and dynamic losses. Switching losses occur due to the transition of switches between on and off states. This can be reduced using low frequency and smaller FET. Dynamic losses occur due to the flow of current through the devices. Decreasing the frequency to reduce the switching losses will increase the size of the inductor and the conduction losses accordingly. Hence a trade off is to be made for the proper choice of the switching frequency and the

components. The losses and expected efficiency are calculated for the designed boost converter. The converter is powered by the solar panel, providing 4.5 V and 213 mA under the insolation of 1000 W/m^2, the switching frequency used is 5 kHz. With this consideration the duty cycle and the power losses are calculated assuming the converter is in continuous conduction mode [16], [15].

Estimated duty cycle is: $D = \frac{V_{out} - V_{in}}{V_{out}} = \frac{5.6 - 4.5}{5.6} = 0.2$ (19)

The output current is calculated as: $I_{out} = I_{in}(1-D)$ =213× (1-0.2) =170.4 mA (20)

a. Estimation of DC conduction losses

It includes the losses incurred in the source, MOSFET, diode, inductor and the output capacitor. The devices used in the converter are IRF 7101, ZLLS410, PLA10AN3030R4R2 and CKR capacitors and the individual loss calculations are given below.

1. **Source:** Loss in the source = $D \times I_{in}^2 \times R_{series}$ = 0.2× (213×10^{-3})^2×443×10^{-3}= 4.09 mW (21)
2. **MOSFET:** Loss in MOSFET = $D \times I_{in}^2 \times R_{dson}$= 0.2× (213×10^{-3})^2×0.10=907.38 µW (22)
3. **Diode loss:** $V_f \times I_{out} + I_{out}^2 \times R_d$ =0.58×170.4m+ (170.4m)^2×0.58= 115 mW (23)
4. **Inductor loss:** $I_{in}^2 \times R_L$ = 213m^2×0.1= 4.5 mW (24)
5. **Output Capacitor loss:** $I_{out}^2 \times R_{esr}$ =1.0554×10^{-3}× (170.4×10^{-3})^2= 21.8 mW (25)
6. **Total conduction losses** =4.09m+907.38µ+115m+4.5m+21.8m = 145.39mW (26)

Eqn. (26) gives the total conduction loss, which is the sum of losses from Eqns (21) to (25).

b. Estimation of Dynamic Losses

These losses are highly influenced by the current flowing through the components and the switching frequency.

1. **MOSFET :** Power loss in gate, $P_{iss} = C_{iss} V_{cg}^2 f_s$ = 320p×3^2×5k=14.4 µW (27)
2. **Output Capacitor loss:** Power loss in discharging, $P_{oss} = 0.5 \times C_{oss} \times V_{Tr}^2 \times f_s$ = 0.5 × 250p × 5.6^2× 5k =19.6 µW (28)
   (in CCM V_{Tr}=output converter voltage)
3. **Switches:** Loss in Transition process, $P_{Tsw} = k \times (t_r I_{Lmax} + t_f I_{Lmin}) V_{out} \times f_s$ = 0.3× (10+30) ×10^{-9} × 213×10^{-3} ×5.6×5000 =71 µW (29)

4. **Diode loss:** $P_{Tdiode} = V_{out} \times \left(I_{Lmin} \times t_{rr} + Q_r \right) \times f_s$ = 5.6× (213.10^{-3}×3.10^{-9}+210.10^{-12}) × 5000 = 23.77 µW (30)
5. **Choke core loss:** $P_{core} = k \times f_s^{\alpha} \times \Delta B^{\beta} \times V_{core}$ = 1× (5×10^{3})$^{1.3}$× (30×10^{-3})$^{2.55}$×5.040×10^{-6} = 42.43 µW (31)
6. **Total dynamic loss**: Dynamic loss is the sum of losses from eqns (27) to (31).

$$P_{dyn} = P_{iss} + P_{oss} + P_{Tsw} + P_{Tdiode} + P_{core} = 14.4\mu + 19.6\mu + 71\mu + 23.77\mu + 42.43\mu = 171.2\mu W \quad (32)$$

The total loss in the converter circuit is the sum of the conduction losses and the dynamic/switching losses. For the designed converter it is equal to 145.6mW. This yields an efficiency of 85%. The working of the solar energy harvester is verified experimentally and the input and output parameter measurements are shown in figure 8. The power is directly measured using single phase clamp on fluke meter at both the input and output sides. The MPPT conversion yields an efficiency of 80% experimentally.

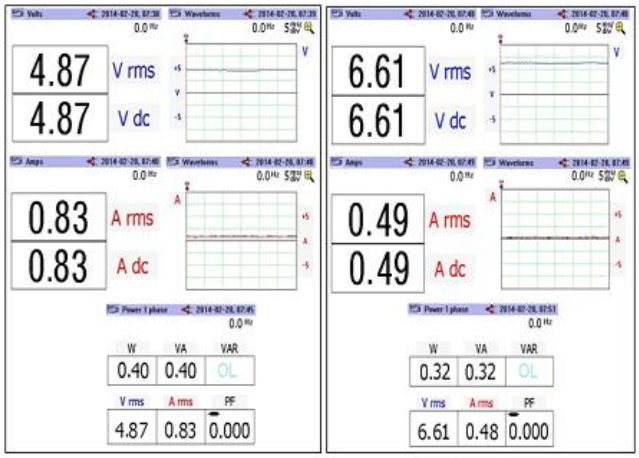

Figure 8. Input and output voltage, current and power measurements

V. DESIGN AND SIZING OF PV PANEL AND BATTERY

The motes are assumed to follow the schedules in the Case I and Case II. It is assumed that in the active period the mote is in idle state for 0.025 % of the on time and for the remaining duration, half of the time in transmit mode and half of the time in receive mode. With this scenario the time

duration spent by the mote in sleep, idle, transmit and receive mode for different duty cycles are calculated. In Case II schedule the mote is assumed to be in active state for 1 %, 10 % and 40 % of its allotted time T_c leading to the duty cycle of 4 %, 5 % and 7 %. With these schedules the solar panel and the battery storage requirements are calculated.

Specifications:

Duration of operation=24 hrs a day

Average time of sunlight available in a day, $T_{sun} = 8hrs$

Number of sunless days per week, $D_{sun\_less} = 2days$

Peak value of insolation = 900 W/m^2

Maximum depth of discharge of a battery=50%

Assumptions:

Electrical efficiency of the circuit of MPPT,

η_{mppt}= 85% and 80% (as calculated in section 4)

Charge/discharge cycle efficiency of the battery, η_{bat}=90 % (new one)

Interconnection loss = 2 %

The single day energy profile of the TelosB mote using SMAC schedule is given in the Table 2. The data is given for 1 % duty cycle operation. The panel requirements for higher duty cycle ratios are also calculated, even though the sensor networks will have a duty cycle mostly less than 1 %. It is to perform worst case analysis of the power requirement. The system designed for 1 % duty cycle is sufficient to handle the loads with duty cycle less than that too. The panel size requirement for the operation of the mote with the mentioned duty cycle is obtained.

Table 2: Single day energy profile for 1 % duty cycle

Mote state	Sleep	Idle	Transmit	Receive
Duration (hrs)	23.75	0.016	0.117	0.117
Power consumption (Watts)	10.2µ	37.6m	39m	43.6m
Energy (J)	242.25µ	601.6µ	4.563m	5.101m

Energy requirement for one day, $E_{day} = E_{sleep} + E_{rx} + E_{idle} + E_{tx}$ = 10.51 mWhr

The energy required for the mote, for one week, $E_{w\_load} = E_{day} \times 7$ = 73.56 mWhr

The energy given directly to the load (battery and mote) in a week, $E_w = E_{day} \times T_{sun} \times \left(7 - D_{sun\_less}\right)$ = 420.4 mWhr

Additional energy available in a week, $E_{rem} = E_w - E_{w\_load}$ = 346.84 mWhr.

The remaining additional energy must be stored in and supplied by the battery bank. For efficient storage in the battery, the battery charge and discharge efficiency has to be taken into account. The energy to be supplied to battery to store an energy level of E_{rem} is calculated as below.

$$E_{req\_bat} = \frac{E_{rem}}{\eta_{bat}} = 385.3 \text{ mWhr}$$

The energy to be supplied is calculated as $E = E_w + E_{req\_bat}$ = 805.7 mWhr

The total energy reaching the battery is supplied by the MPPT, hence the MPPT power converter efficiency (85%) must be included in the energy requirement. The energy requirement after including the MPPT efficiency is as follows,

$$E_{mppt} = \frac{E}{\eta_{mppt}} = 947.92 \text{ mWhr}$$

The total energy required from the solar panel is calculated with including the wiring and cable losses.

$E_{total} = E_{mppt} + \left(E_{mppt} \times loss\%\right)$=995.31 mWhr

The total energy required is to be generated by the module in $\left(7 - D_{sun\_less}\right)$ days with T_{sun} hours of sunlight on each day. So the power of the module is given as,

$$P_{module} = \frac{E_{total}}{\left(7 - D_{sun\_less}\right) \times T_{sun}} = 24.88 \text{ mW}$$

The module used is SL8585mm, with peak power of 950mW. The panel is rated at 1000 W/m^2 and it will not provide peak power all the time as it mainly depends on the insolation and the temperature. This approximation has to be included to the power required.

Approximation, $P_{approx} = P_{panel\_max} \times 0.635$= 603.25 mW

The final power required from the module is given by,

$$P_{final} = P_{module} \times \frac{P_{panel\_max}}{P_{approx}} = 39.18 \text{ mW}$$

Similarly the calculations are done for different duty cycles with the theoretical (datasheet) and practical (measured) values of energy consumption and the panel rating required for SMAC and TDMA-MAC based mote operation are shown in figure 9.

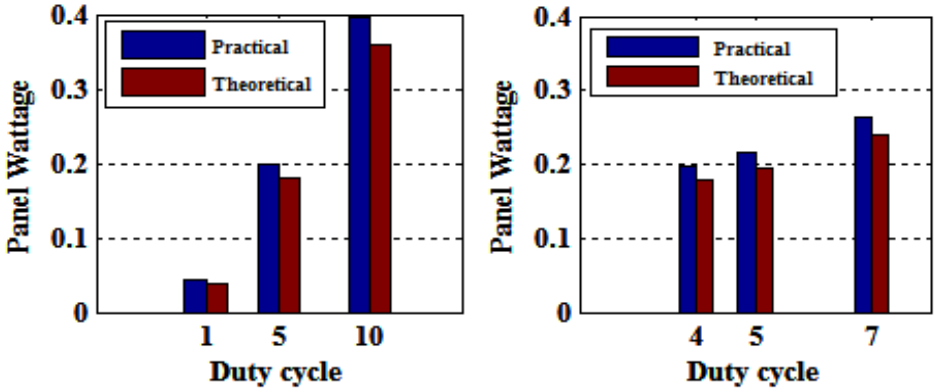

a) SMAC schedule b) TDMA-MAC schedule

Figure 9. Panel rating required for the a) SMAC schedule and b) TDMA-MAC schedule under varying duty cycles of the mote

TelosB mote requires 183.7 mW range panel when modeled using theoretical values of the current consumption, whereas in practical case it needs 203 mW panel at 4 % duty cycle with TDMA MAC schedule. Similarly in SMAC schedule, TelosB mote requires 39.18 mW and 43.34 mW in theoretical and practical scenario. It is clear that the panel rating required is larger for all cases in practical than the theoretical scenario. Hence the panel rating cannot be chosen based on the theoretical calculation alone; they must have a marginal value to accommodate this variation. In both schedules on an average 10.5 % increase in panel rating is obtained in practical calculation. Hence it is suggested to add a marginal value of 10 % than the calculated value for the panel rating calculations to meet the real time requirements.

a. Size of the battery bank

If the voltage of the battery bank is 4.8 V, then its charge capacity is 531.5/4.8= 110.73 mAhr, since batteries must retain 50 % of the charge after supplying the required energy, their charge holding capacity must be twice this value.

Total charge required = 110.73×2=221.46 mAhr

Single cell of NiMH with 150 mAh capacity have a terminal voltage of 1.2 V each [26]. To get 4.8 V, 4 such cells must be connected in series. We have characterized the battery requirement using the 4.8 V, 150 mAh NiMH battery. To increase the capacity, batteries should be connected in parallel. Hence to satisfy the above charge requirement two 4.8 V, 150 mAh NiMH batteries has to be connected in parallel. Similarly the charge capacity required and the number of batteries required is calculated for different duty cycles and different motes, the results are shown in figure 10.

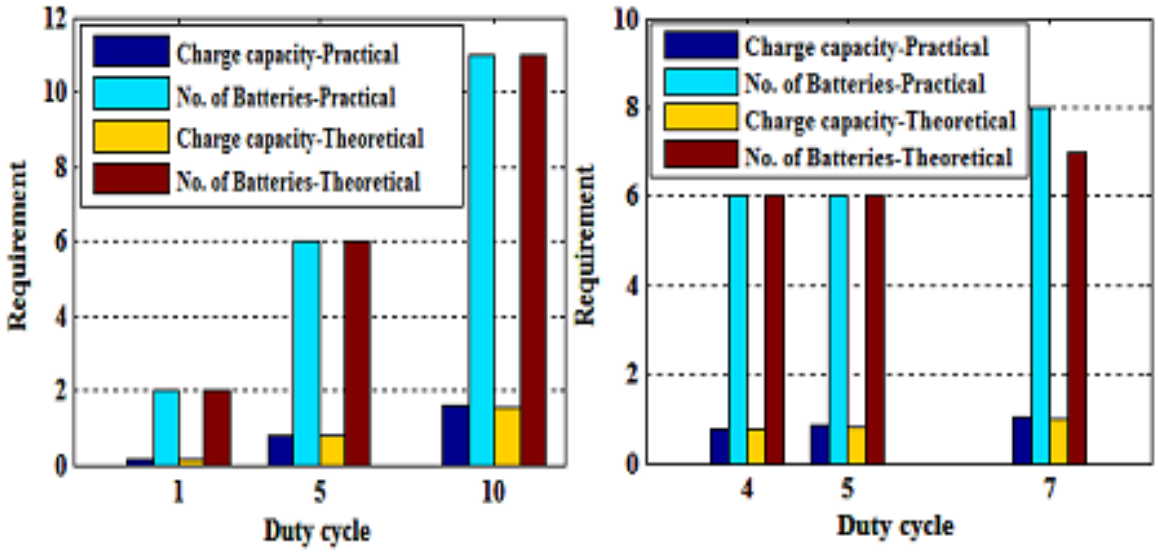

a) SMAC schedule b) TDMA-MAC schedule

Figure 10. Required charge capacity of the battery and number batteries required for the SMAC and TDMA-MAC schedules under varying duty cycles of the mote

TelosB mote with SMAC schedule requires 160.54 mAh charge capacity at 1 % duty cycle whereas with TDMA MAC schedule requires 752.7 mAhr. The practical values obtained for the same scenario is 167.16 mAhr and 783.01 mAhr respectively. Though the practical calculation requires 4 % additional charge capacity on an average, the number of batteries remained the same for all cases except the 7 % duty cycle scenario of TDMA MAC schedule. Hence the battery choice can be made based on the theoretical calculation, as it is not much deviated from the practical requirement.

VI. LIFETIME ANALYSIS WITH ENERGY HARVESTER

The lifetime of the mote depends on the cycle life, recharge rate of the battery with varying illumination and discharge capacity of the battery [26], [4]. The lifetime prediction is done with the mote transmitting 16 bytes of data during every frame in the SMAC slot assignment. The parameters assumed are T_{idle}= 3 ms, T_{rx}= 5 ms, T_{tx}= 9 ms and T_{sleep}=1.5 s (D=1.1%). The linear prediction model for the SOC [4], [5] has been used in this paper to determine the SOC of the battery efficiently. The prediction is done using MATLAB SIMULINK. The average current delivered by the battery during one frame is calculated using Eq. 33, where q is the charge consumed by the load over frame duration. Charge consumed depends on the states of operation of the mote. Here the mote is assumed to be in transmit, receive, idle and sleep states during every frame duration. This determines the rate at which the battery is discharged.

$$I_{avg} = \frac{q}{T_{frame}} \tag{33}$$

The recharge rate of the battery is calculated by charging the battery from the solar harvester while the load is disconnected. The state of charge of the battery (SOC) during the recharge process is calculated from the discharge time. Starting from the cut-off state (50 % of its original capacity), the battery is recharged under fixed light conditions for specific time. The battery is then discharged at a fixed rate until the cut-off circuit disconnects the load. The number of transmissions performed during the discharge time T_d, is used to compute the State of Charge of the battery. The test is repeated with different recharge time. The state of charge is plotted and is shown in figure 11.

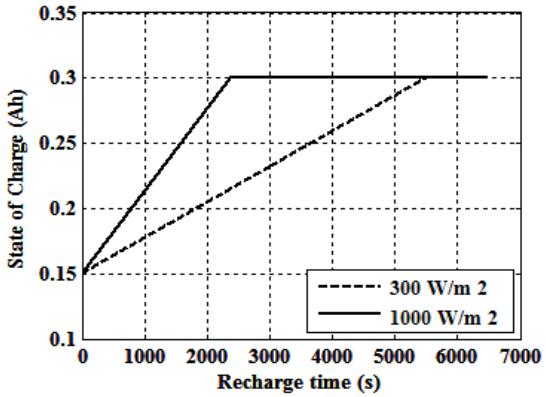

Figure 11. Battery state of charge

The rate of recharge parameter (β) is obtained from the slope of the state of charge curve. The discharge capacity is assumed to be constant with the battery discharge current lesser than 110 mA [4], [5]. The discharge and recharge process is characterized with constant parameters (I_{avg} and β) over the frame duration, the SOC is computed using a linear model [26]. The SOC of the battery for the next n frames is calculated using the Eq. 34. where I_{sd} is the self discharge current of the battery. The lifetime of the mote following the two schedules is predicted and is given in the Table 3. and Table 4.

$$SOC(t + nT_{frame}) = SOC(t) + \beta \times T_{sun} - I_{avg} nT_{frame} - I_{sd} nT_{frame} \quad (34)$$

Table 3: Lifetime prediction of the mote using SMAC schedule

Illumination (W/m^2)	β **(mA)**	T_{frame}=1.517s $I_{avg} = 229.76$ µA	T_{frame}=1.517 s $I_{avg} = 236.39$ µA
		Lifetime-theoretical values (days)	**Lifetime - Measured values (days)**
100	59.4	141	137
200	91.8	188	182
300	108	211	205
400	129.6	242	236
500	151.2	274	266
600	172.8	305	297
700	183.6	321	312
800	194.4	336	327
900	205.2	352	342
1000	226.8	383	373

In SMAC schedule the average current consumption of the TelosB mote using the theoretical and measured current consumption details is 229.76 µA and 236.39 µA respectively. The recharge rate of the battery with the provided illumination is calculated individually for all the ranges between 100 to 1000 W/m^2 of insolation. Using the Eqn 24, the life time of the mote is predicted and is given below. Without harvester, TelosB mote following SMAC schedule will last for 54 (as per datasheet) and 53 (as per measurement) days based on the current consumption. Whereas,

if harvester is used and minimum insolation is available, the lifetime is nearly doubled. With maximum insolation level the lifetime increases by 6 % on an average. For this scenario the insolation is assumed to be available for 8 hours, calculation is done for a single recharge cycle of the battery. If the lifetime of the battery is considered, the lifetime of the mote will increase to a greater extent in both cases.

The lifetime prediction is done with the mote transmitting 16 bytes of data during every frame in the TDMA-MAC slot assignment. The parameters assumed are T_r =14.3 s, T_{idle}= 3 ms, T_{rx}= 5 ms, T_{tx}= 3 ms and T_{sleep}=14.289 s (D<0.1 %). In TDMA-MAC schedule the average current consumption of the mote is 20.75 µA and 22.49 µA under theoretical and measured analysis respectively. With no harvester TelosB motes following TDMA-MAC schedule will last for 555.8 days respectively. Whereas if the harvester is used and minimum insolation is available, the lifetime is nearly tripled. With maximum insolation level the lifetime increases by 6 %. For this scenario the insolation is assumed to be available for 8 hours.

Table 4: Lifetime prediction of the mote using TDMA-MAC schedule

Illumination (W/m^2)	β **(mA)**	T_{round} =14.3 s, I_{avg} = 20.75 µA **Lifetime-theoretical values (days)**	T_{round} =14.3 s, I_{avg} = 22.49 µA **Lifetime - Measured values (days)**
100	59.4	1556	1441
200	91.8	2077	1923
300	108	2337	2164
400	129.6	2684	2486
500	151.2	3031	2807
600	172.8	3378	3128
700	183.6	3551	3289
800	194.4	3725	3449
900	205.2	3898	3610
1000	226.8	4245	3931

The lifetime of TelosB mote is calculated with the required light level and is shown in Table 5.

Table 5: Expected Life Time of TelosB Mote

Duty Cycle	Required Light/ Month	Life Time-Theoretical values	Lifetime-Measured values
1.1%	8 hrs	44.35 yrs	43.11 yrs
	5 hrs	31.03 yrs	30.16 yrs
	1 hr	13.25 yrs	12.89 yrs

With 1.1 % duty cycle mote can continue its operation to 43 years with 8 hours of available sunlight per month. The WSN applications have duty cycle less than 1.1 %, which also confirms the perpetual operation of the motes with the energy harvester.

VII. CONCLUSION

In this paper a detailed methodology to analyze the energy consumption and lifetime prediction for wireless sensor motes have been derived with TelosB mote as an example. The analysis has been presented for the mote with and without energy harvester. The simulations proved that the lifetime of the motes increased by nearly 1.6 % to 6 % based on the insolation available from the sun, for single recharge cycle of the battery. The panel sizing requirement, battery charge capacity required and the number of batteries required to provide the necessary charge capacity, have also been presented for different schedules with varying duty cycles. The harvester requirements have been calculated with the physical modeling of the harvester blocks. The TelosB mote requires 8 hours of sunlight per month to achieve a lifetime of 44 years. The obtained results are validated with the values calculated using real time measurement of current consumption of the mote. The expected lifetime reduces by 0.02 % in real time when compared to the theoretical calculation. Hence the motes with energy harvester are capable of prolonging the lifetime of the network to greater extent. It is also suggested to choose the panel with its rating equal to 10.5 % more than the panel rating calculated theoretically. Moreover this paper helps any user to design a proper energy harvesting circuit, sizing of PV panel, battery sizing etc. for wireless sensor networks. Lifetime prediction of the mote can be extended with solar panels of different technologies, leading to sensitivity analysis of the panel parameters.

REFERENCES

[1] F. Akyildiz, W. Su, Y. Sankarasubramaniam and E. Cayirci, "'Survey of Sensor Networks," *IEEE Communications Magazine*, vol.40, no.8, pp.102-114, 2002

[2] Ian F., Akyildiz, Tommaso Melodia and Kaushik R.Chowdhury, "A Survey on wireless multimedia sensor networks," *Computer Networks the International Journal of Computer and Telecommunications Networking*, vol.51, no.4, pp.921-960, March 2007.

[3] Abhiman Hande, Todd Polk, William Walker, Dinesh Bhatia., "Indoor Solar Energy Harvesting for Sensor Network Router Nodes," *J. Microprocessors & Microsystems*, vol.31, no.6, pp.420-432, Sep 2007.

[4] Andrea Castagnetti, Alain Pegatoquet, Cecile Belleudy and Michel Auguin, "A framework for modeling and simulating energy harvesting WSN nodes with efficient power management policies," *EURASIP Journal on Embedded Systems*, vol.2012, no.1,pp. Dec 2012.

[5] Andrea Castagnetti, Alain Pegatoquet, C´ecile Belleudy and Michel Auguin, "An Efficient State of Charge Prediction Model for Solar Harvesting WSN Platforms," in *Proc. of 19th International conference on Systems, Signals and Image Processing*, Vienna, Austria, pp.122-125, April 2012.

[6] Aredes M, França B, and Aredes M, "Fuzzy Adaptive P&O Control for MPPT of a Photovoltaic Module," *Journal of Power and Energy Engineering*, vol. 2, 120-129, 2014.

[7] H. Al-Abri, S.C. Mukhopadhyay, G. A. Punchihewa, N. Suryadevara and Y. M. Huang, "Comparison of applying Sleep Mode function to the Smart Wireless Environmental Sensing Stations for Extending the Life time," in *Proc. of IEEE I2MTC 2012 conference*, Graz, Austria, pp. 2634-2639, 2012.

[8] Babaa S, Armstrong M, and Pickert V, "Overview of Maximum Power Point Tracking Control Methods for PV Systems," *Journal of Power and Energy Engineering*, vol. 2, pp.59-72, 2014.

[9] Blue Solar SL8585mm, Solar Panel, http://www.xscyz.com/, accessed on May 2014.

[10] Cesare Alippi and Cristian Galperti, "An Adaptive System for Optimal Solar Energy Harvesting in Wireless Sensor Network Nodes," *IEEE Trans Circ Syst*, vol.55, no.6, pp.1742-1750, July 2008.

[11] Chien-Ying Chen and Pai H. Chou, "DuraCap: a Supercapacitor-Based, Power-Bootstrapping, Maximum Power Point Tracking Energy-Harvesting System," in *Proc.of 2010 ACM/IEEE International Symposium on Low-Power Electronics and Design (ISLPED)*, Austin, TX, USA, pp.313-318, August 18-20, 2010.

[12] Chulsung Park and Pai H. Chou., "Ambimax: Autonomous Energy Harvesting Platform for Multi-Supply Wireless Sensor Nodes," in *Proc.of 3rd Annual IEEE Communications Society on Sensor and Ad Hoc Communications and Networks conference*, California, pp.168-177, 2006.

[13] S.J. Chiang, H.J. Shieh and M.C., Chen, "Modeling and Control of PV Charger System with SEPIC Converter," *IEEE Transactions on Industrial Electronics*, vol.56, no.11, pp.4344-4353, 2009.

[14]Davide Brunelli, Clemens Moser, Lothar Thiele and Luca Benini, "Design of a Solar-Harvesting Circuit for Batteryless Embedded System," *IEEE Trans Circ Syst*, vol.56, no.11, pp.2519-2528, Nov 2009.

[15]R.Erickson, D.Maksimovic, *Fundamentals of power electronics*, Kluwer Academic, Massachusetts, 2000.

[16]Eichhorn Travis, "Boost Converter Efficiency through Accurate Calculations," *Power Electronics Technology*, vol.34, no.9, pp 30-35, Sep 2008.

[17]Ganti Raghu K., Praveen Jayachandran, Haiyun Luo and Tarek F. Abdelzaher**,** "Data link Streaming in Wireless Sensor Networks," in *Proc.of 4th International conference on Embedded networked sensor systems, ACM SenSys*, New York, USA, pp. 209-222, Nov 2006.

[18]HadiMalek and YangQuan Chen, "BICO MPPT: A Faster Maximum Power Point Tracker and its Application for Photovoltaic Panels," *International Journal of Photoenergy*, Vol. 2014, Article ID 586503, 9 pages.

[19]Hoonki Kim, et.al, "A 1-mW Solar-Energy-Harvesting Circuit Using an Adaptive MPPT With a SAR and a Counter," *IEEE Trans Circ Syst-II,*vol.60, no.6,pp.331-335, June 2013.

[20]R.Hemalatha, R.Ramaprabha, S.Radha, "Modeling of Photovoltaic Charging System for the Battery Powered Wireless Sensor Networks," in *Proc.of Third International Conference on Trends in Information Telecommunication and Computing, Lecture notes in Electrical Engineering*, vol.150, pp. 225-235, 2013.

[21]Z.Ivanovic, B.Blanusa, M.Knezic, "Power Loss Model for Efficiency Improvement of Boost Converter," in *Proc.of XXIII International Symposium on Information, Communication and Automation Technologies*, Sarajevo, Oct 27-29, 2011.

[22]Joseph Polastre, Robert Szewczyk and David Culler, "Telos: Enabling Ultra-Low Power Wireless Research" in *Proc.of 4th international symposium on Information processing in sensor networks*, LOS Angeles, CA, pp. 364-369, April 2005.

[23]A.Lay-Ekuakille, G. Vendramin, A. Fedele, L. Vasanelli and A. Trotta, "PV Maximum Power Point Tracking Through Pyranometric Sensor: Modelling and Characterization," *International Journal on Smart Sensing and Intelligent Systems,* Vol. 1, No. 3, pp.659-678, 2008.

[24]Liu, C.-L, Chen, J.-H, Liu, Y.-H, Yang, Z.-Z, "An Asymmetrical Fuzzy-Logic-Control-Based MPPT Algorithm for Photovoltaic Systems," *Energies*, vol.*7*, 2177-2193, 2014.

[25]MATLAB and Simulink for technical computing, www.mathworks.in, accessed on May 2014.

[26]NiMH battery datasheet, www.rapidonline.com. accessed on May 2014.

[27]C. Ranhotigamage and S. C. Mukhopadhyay, "Field Trials and Performance Monitoring of Distributed Solar Panels using a Low Cost Wireless Sensors Network for Domestic Applications," *IEEE Sensors Journal*, Vol. 11, No. 10, pp. 2583-2590, 2011.

[28]C. Ranhotigamage, S.C.Mukhopadhyay, S.N.Garratt and W.M.Campbell, "Measurement and Monitoring of Performance Parameters of Distributed Solar Panels using Wireless Sensors Network," in *Proc. of IEEE I2MTC 2011 conference*, Hangzhou China, pp. 1567-1572, 2011.

[29]C. Ranhotigamage, S.C.Mukhopadhyay, S.N.Garratt and W.M.Campbell, "Wireless Performance Monitoring of Distributed Solar Panel Networks," in *Proc. of 2010 International Digital Signal Processing Creative Design Contest*, Taiwan, pp. 44-49, 2010.

[30]S.Sanka and G. Konchady, "Communication between Wireless Sensor Devices and GNU Radio," May 2009.

[31]G.Shafiullah, A.Thompson, Wolfs, Peter, S .Ali, "Energy-Efficient TDMA MAC Protocol for Wireless Sensor Networks Applications," in *Proc. of International Workshop on Internet and Distributed Computing Systems*, Khulna, Bangladesh, pp. 85-90, Dec 2008.

[32]Shubhajit Roy Chowdhury, Dipankar Mukherjee and Hiranmay Saha, "FPGA based Maximum Power Point Tracker of Partially Shaded Solar Photovoltaic Arrays using Modified Adaptive Perceptive Particle Swarm Optimization," *International Journal on Smart Sensing and Intelligent Systems*, Vol. 2, no. 4, 661-675, 2009.

[33]Takao Kikuoka and Hiroaki Yamamoto, "System for measuring state of charge of storage battery," US Patent 4377787, March 1983.

[34]Ting CAO, Yuhao WANG, Xinmin XIONG and Yan HAO,"Cluster-based Routing Performance Optimization Constraint of Energy, Delay and Connectivity Metrics in Wireless Sensor Network," *International Journal on Smart Sensing and Intelligent Systems*, Vol. 6, No. 5, pp.2103-2118, 2013.

[35]Trishan Esram and Patrick L. Chapman, "Comparison of Photovoltaic Array Maximum Power Point Tracking Techniques," *IEEE Transactions on Energy Conversion*, vol.22, no.2, pp.439-449, June 2007.

[36]Wei Ye, John Heidelmann and Deborah Estrin, "Energy efficient MAC protocol for wireless sensor networks," in *Proc.of IEEE Infocom*, New York, USA, pp. 1567-1576, June 2002.

[37]Wei Ye, John Heidelmann and Deborah Estrin., "Medium Access control with coordinated adaptive sleeping for wireless sensor networks," *IEEE/ACM trans. on Networking*, vol.12, pp. 493-506, June 2004.

[38]Xiaofan Jiang, J.Polastre and D.Culler, "Perpetual environmentally powered sensor networks**,"** in *Proc. of Fourth International Symposium on Information Processing in Sensor Networks*, pp.463-468, April 15, 2005.

[39]Ying Guo, Feng Hong and Zhongwen Guo, "Duty Cycling in Target Monitoring Wireless Sensor Network Systems," *International Journal on Smart Sensing and Intelligent Systems*, Vol. 6, No. 3, pp.1054-1076, 2013.